Available online at www.sciencedirect.com
ScienceDirect
European Journal of Mechanics B/Fluids 27 (2008) 62–74

Numerical solutions of the Boltzmann equation: comparison of different algorithms

Piotr Kowalczyk [a,*], Andrzej Palczewski [a], Giovanni Russo [b], Zbigniew Walenta [c]

[a] *Institute of Applied Mathematics, Warsaw University, Banacha 2, 02-097 Warszawa, Poland*
[b] *Università di Catania, Viale Andrea Doria 6, 95125 Catania, Italy*
[c] *Institute of Fundamental Technological Research, Polish Academy of Science, Swietokrzyska 21, 00-049 Warszawa, Poland*

Received 11 September 2006; received in revised form 23 March 2007; accepted 5 April 2007

Available online 24 April 2007

Abstract

In the paper we compare different algorithms for numerical solutions of the Boltzmann equation. For this comparison we have taken the standard problem of the shock wave structure in a mono-atomic rarefied gas. Different parameters characterizing the shock structure have been calculated by a Monte Carlo simulation (DSMC), a second order time-relaxed Monte Carlo method (TRMC2), a fully deterministic discrete velocity method (DV), a discrete velocity method with Monte Carlo calculations of collision integral (DVMC) and a molecular dynamics method (MD). Results of these calculations have been compared with the shock wave structure obtained in experiments in a shock tube. The results of the comparison are not conclusive. We have observed general agreement between numerical and experimental results but there is no single numerical method which fits best to the experimental measurements.

Keywords: Boltzmann equation; Numerical methods

1. Introduction

Numerical solutions of kinetic equations of Boltzmann type have been known for more than 40 years. Nevertheless a construction of an accurate numerical solution to the Boltzmann equation still presents a difficult task. This is mostly caused by a high dimensionality of the equation and in particular its non-linear collision part. Due to the complexity of the numerical problem the only accessible numerical algorithm was based for a long time on Monte Carlo techniques. However, increasing computational power of modern computers opened the possibility for developing new algorithms. In the last decade a number of new computational methods for solving the Boltzmann equation has been developed. Some of these methods have better approximation properties than the old Monte Carlo based methods. A natural question which arises when we compare different numerical algorithms is "which of the methods under investigation performs better in real calculations". This question should be sharply distinguished from the theoretical (mathematical)

* Corresponding author.
E-mail addresses: pkowal@mimuw.edu.pl (P. Kowalczyk), apalczew@mimuw.edu.pl (A. Palczewski), russo@dmi.unict.it (G. Russo).

0997-7546/$ – see front matter
doi:10.1016/j.euromechflu.2007.04.001

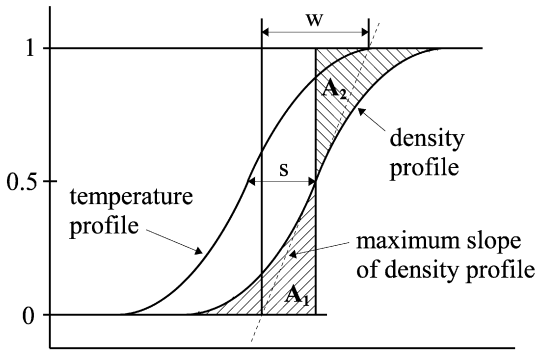

Fig. 1. Shock wave structure and characteristic parameters.

properties of the compared algorithms as it is well known that in many cases methods with very good theoretical properties perform poorly in practical calculations.

The aim of this study is the comparison of several numerical methods of solution of the Boltzmann equation. Usually, in order to compare different numerical methods, we perform a number of simulations which give us the information about numerical stability and numerical rate of convergence. It is often very difficult to draw a conclusion about the accuracy of obtained numerical results. To get such information we can compare numerical solutions with the exact solution of the problem. As exact solutions are very rare and usually restricted to simple cases, our knowledge about accuracy is also rather limited. To overcome this difficulty we decided to compare numerical results with experimental data.

To set up an experimental regime in which gas flow can be adequately described by the Boltzmann equation is rather difficult. It corresponds to a highly rarefied gas, possibly of noble type to eliminate additional degrees of freedom, and there are not too many experimental data of such problems available. One of the classical rarefied gas problems is a shock tube problem in which a planar shock wave is generated. This problem is easy for numerical simulation as there is one space dimension (and three velocity dimensions) in the problem. Fortunately we have got access to highly accurate experimental data obtained by one of the authors at the laboratory of the Institute of Fundamental Technological Research in Warsaw.

The shock wave structure is a classical problem of rarefied gas dynamics. It has been investigated by many different numerical methods and a number of different shock wave characteristics has been recognized. The most popular and widely used is the shock wave thickness. But some more sophisticated parameters have also been used.

In [1] the shock wave structure is predicted by the hydrodynamic approach. The author solves the full Burnett equations and compares the solution with Navier–Stokes results and experimental data using inverse density thickness as a measure of the structure of the shock. The simple density, velocity and temperature profiles of the shock are used in [2] to compare the solution of the Navier–Stokes equations, DSMC and so-called quasi-gasdynamics equations developed by the authors.

Following Muntz et al. [3], for our comparison work we have chosen the following quantities as the characteristic parameters of the shock structure: a maximum-slope shock thickness w measured on density profile, a shift between temperature and density scaled profile s and a geometric shape factor $Q = A_1/A_2$, which measures asymmetry of the density profile (cf. Fig. 1 for the precise definitions of these parameters).

Note that the length scale is measured in units of mean free path (see Section 3.1) and therefore all such parameters are expressed by non-dimensional numbers.

2. Experimental data

2.1. Experimental setup

Accurate measurements of shock wave structure required the apparatus suitable for low-density measurements. The shock tube of the Institute of Fundamental Technological Research, Polish Academy of Sciences, Warsaw, was employed for this purpose. This tube [4], of 250 mm internal diameter and 17 meters long, made it possible to work

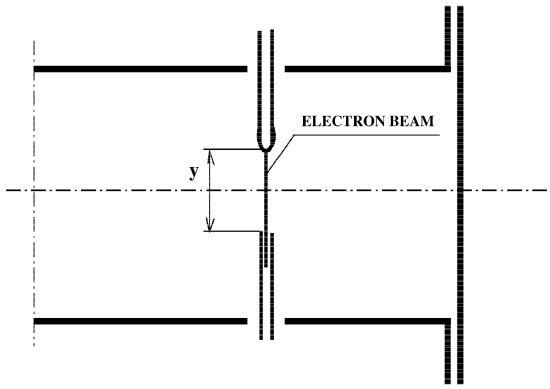

Fig. 2. Test section of the shock tube with electron beam densitometer.

at densities, corresponding to the gas particles mean free path of about 1 mm, without noticeable influence of the wall boundary layers. Fig. 2 shows a schematic drawing of the test section of the shock tube.

The distribution of the gas density inside the shock was measured with the standard, electron beam attenuation technique [5]. This technique employs the attenuation of the beam due to scattering of electrons colliding with gas molecules. The beam was placed perpendicularly to the tube axis in such a way, that only the central part of the flow was used for measurements (Fig. 2). The beam length y between the injecting needle and the Faraday cage was equal to only about 35 millimeters. This was because in the low-density shock tube the shock wave is always at least slightly curved due to the influence of the wall boundary layer; only the central part of the shock may be considered sufficiently plane for measurements.

2.2. Data evaluation procedure

During the test run, the beam current at the inlet to the test section (outlet from the injecting needle) is kept constant. If the gas density and the electron scattering cross-section are constant along the beam, the dependence of the attenuated beam current i upon gas density ρ has the form

$$\frac{i}{i_0} = \exp(-ky\rho)$$

where i_0 is the beam current at the inlet to the tube, k – the beam attenuation coefficient (proportional to the electron scattering cross-section) and y – the beam length.

Since it is difficult to measure accurately the values i_0 and k, we make use of the fact, that the densities ρ_1 in front of the shock and ρ_2 behind it, are known and the corresponding values of the attenuated beam current, i_1 and i_2, are registered in each run. We can eliminate i_0 and kx and obtain the explicit dependence of ρ on i

$$\frac{\rho - \rho_1}{\rho_2 - \rho_1} = \frac{\ln(i/i_1)}{\ln(i_2/i_1)}.$$

2.3. Conditions of experiment

The conditions of experiment were selected as follows:

- Argon (spectrally pure) was used as the test gas.
- The shock Mach number M was equal to 2.80 ± 0.08.
- The initial pressure was equal to 7.33 ± 0.15 Pa.
- The initial temperature was equal to the room temperature, 298 ± 3 K.

For such conditions the mean free path for argon is about 0.95 mm and the maximum slope shock thickness about 4 mm (cf. [6]). At such shock thickness it was possible to obtain reliable results with an electron beam 0.5 mm thick.

2.4. Accuracy

The inaccuracy of the density measurement was estimated to be about ±2.5% of the difference between the final and initial values. The main source of errors was the inaccuracy of setting the initial parameters, mainly pressure (±2%). The inaccuracy of setting the Mach number (±0.5%), at its selected value of 2.8, had negligible influence upon the overall accuracy of the measurements. The inaccuracy due to finite electron beam thickness, most serious in the places of the largest curvature of the shock structure diagram, was estimated not to exceed 0.1%.

3. Numerical methods

3.1. The Boltzmann equation

Our aim is to find the shock wave structure obtained in the physical experiment by solving a relevant problem for the Boltzmann equation. To this end we consider the Boltzmann equation in a 3-dimensional space for the distribution function $f(x, v, t)$

$$\frac{\partial f}{\partial t} + v\frac{\partial f}{\partial x} = Q(f, f).$$

We restrict ourselves to the model of hard sphere particles. Then the collision term $Q(f, f)$ has the form

$$Q(f, f) = \int_{R^3}\int_{S^2} u\sigma\big(f(v')f(w') - f(v)f(w)\big)\,\mathrm{d}w\,\mathrm{d}n$$

where v and w are pre-collision velocities, and the post-collision velocities v' and w' are given by the expression

$$v' = \frac{1}{2}(v + w + un), \qquad w' = \frac{1}{2}(v + w - un)$$

with $u = |v - w|$ and $\sigma = d^2/4$.

In these formulas n is the outer unit vector on the sphere S^2 and d is the diameter of particles (hard spheres).

We express the above Boltzmann equation in the dimensionless variables appropriate for the shock wave structure

$$\bar{x} = \frac{x}{L}, \quad \bar{v} = \frac{v}{\nu_0}, \quad \bar{t} = \frac{t}{\tau_0}, \quad \bar{f} = \frac{\nu_0^3}{\varrho_0} f$$

where $\nu_0 = \sqrt{2RT_0}$ is the most probable velocity, R – the reduced gas constant, which is the universal gas constant divided by the molecular weight of the gas, $\tau_0 = L/\nu_0$, L – the characteristic dimension, T_0 and ϱ_0 – the temperature and density of the upstream gas.

In these new variables the Boltzmann equation has the form (we skip bars over variables)

$$\frac{\partial f}{\partial t} + v\frac{\partial f}{\partial x} = \frac{1}{4\sqrt{2}\pi Kn}\tilde{Q}(f, f)$$

where $Kn = \lambda_0/L$, $\lambda_0 = 1/(\sqrt{2}\,\pi\varrho_0 d^2)$ is the mean free path and

$$\tilde{Q}(f, f) = \int_{R^3}\int_{S^2} u\big(f(v')f(w') - f(v)f(w)\big)\,\mathrm{d}w\,\mathrm{d}n.$$

Assuming $L = \lambda_0$, i.e. $Kn = 1$, we get the dimensionless Boltzmann equation in which x is in the units of mean free path, velocity in the units of ν_0 and time in the units of τ_0.

In these units the Maxwell distribution function for upstream gas has the form

$$f_M = \frac{\varrho}{\sqrt{\pi^3}}\exp\big(-v^2\big).$$

3.2. Numerical experiment

To calculate a shock wave structure we have designed the following numerical experiment. We consider a constant speed gas flow toward a perpendicular planar wall. The shock wave is generated in the process of gas reflection from this wall. Hence the shock structure is formed in the reflected gas flow. The whole flow is described in a coordinate system attached to the downstream gas. Then the corresponding Rankine–Hugoniot conditions [7] are as follows

$$\tilde{u}_1 = \frac{2}{\gamma+1}\left(M - \frac{1}{M}\right),$$
$$\frac{p_1}{p_0} = \frac{1}{\gamma+1}\left(2\gamma M^2 - \gamma + 1\right),$$
$$\frac{T_1}{T_0} = 1 + \frac{2(\gamma-1)}{(\gamma+1)^2}\left(M^2-1\right)\left(\gamma + \frac{1}{M^2}\right)$$

where $\gamma = 5/3$ is the polytropic constant for a monoatomic gas, p_0, T_0 and p_1, T_1 represent the pressure and temperature in the upstream and downstream, respectively, and $\tilde{u}_1$ is the relative gas velocity, i.e. $\tilde{u}_1 = u_1 - u_0$.

3.3. The splitting method

The classical procedure of solving numerically the Boltzmann equation consists in splitting the equation into the transport and collision steps. Suppose that the solution has to be calculated in the time interval $[0, T]$. We divide interval $[0, T]$ onto N equal subintervals of length $\Delta t = T/N$. Assume that the value f^k of the approximate distribution function f on the time interval $((k-1)\Delta t, k\Delta t]$ has been already computed ($f^0 = f_0$ is the initial distribution function). Then f^{k+1}, the value of the distribution function on the next time interval $(k\Delta t, (k+1)\Delta t]$, is obtained in two steps. In the first step, one solves the free flow problem

$$\frac{\partial f^*}{\partial t} + v \cdot \frac{\partial f^*}{\partial x} = 0 \quad \text{on } \big(k\Delta t, (k+1)\Delta t\big],$$
$$f^*(k\Delta t) = f^k(k\Delta t). \tag{1}$$

The solution of (1) evaluated at the endpoint $(k+1)\Delta t$ serves then as the initial value for the second step which corresponds to the spatially uniform relaxation problem

$$\frac{\partial f^{**}}{\partial t} = Q(f^{**}, f^{**}) \quad \text{on } \big(k\Delta t, (k+1)\Delta t\big],$$
$$f^{**}(k\Delta t) = f^*\big((k+1)\Delta t\big). \tag{2}$$

Finally, using the solution of (2) one sets

$$f^{k+1} = f^{**}\big((k+1)\Delta t\big).$$

Hence, the approximation f on the time interval $(k\Delta t, (k+1)\Delta t]$ is defined by

$$f(t) = f^{k+1}(t) \quad \text{for } t \in \big(k\Delta t, (k+1)\Delta t\big].$$

The boundary conditions appropriate for the particular problem have to be taken into account when solving the free flow stage (1) of the splitting procedure.

3.4. Direct Monte–Carlo simulation

For the DSMC calculations the standard Bird's procedure [8] was employed. To simulate the particles, the Hard Sphere (HS) model was used. Selection of particles for collision was performed with the ballot-box scheme, as proposed by Yanitskiy [9,23].

The calculations were carried on in 1-dimensional geometry. The dimension of each cell in the direction of the shock wave motion was equal to $\lambda_0/4$. The total number of cells was 1600. The initial number of particles was 8000. The number of calculation runs, taken for averaging the results, was equal to 1200.

The selected dimension of the cells seems appropriate for the problem, as the maximum-slope thickness of the shock in a non-ionized gas is never less than about 3 mean free paths in front of it (cf. [6]).

The initial flow velocity toward the reflecting wall was taken equal to 1.6725. This produced the shock wave with shock Mach number equal to 2.8–the value suitable for comparison with the experiment described above.

3.5. Time-relaxed Monte Carlo method

We have used a second order time-relaxed Monte Carlo method (TRMC2) (cf. [10]). This technique, particularly useful when some regions of the flow are not far from the local thermodynamic equilibrium, is based on a formal expansion of the solution of the Boltzmann equation (Wild sums), and on the sampling a certain fraction of particles from a Maxwellian.

Two computations are performed by TRMC scheme. In both cases, the second order version TRMC2 has been used. The first one is a stationary calculation performed in the shock reference frame. The initial condition was the Riemann problem satisfying Rankine–Hugoniot conditions, centered in the middle of the computational domain. The stationary solution is obtained by solving the time dependent Boltzmann equation, and waiting for a time long enough, so that the solution has reached a stationary configuration. The time dependent Boltzmann equation has been solved up to time 100, while statistics has been accumulated after time 10 (which is approximately the time to form a steady shock). The number of space cells used in computations was 1600. The number of particles per cell was 18 upstream and 91 downstream, for a total of 87 200 particles in the computational domain at the beginning of the calculations.

A second computation is performed, by solving the time dependent Boltzmann equation describing particles hitting a wall. The setup is the same as the one used in DSMC. Specular reflection is used at the wall. The computation is carried on up to time $t = 20$. A hundred space cells have been used, with 100 particles per cell at the initial time. The run is repeated 500 times, with different seeds for the random number generator, and the various results are averaged, in order to reduce statistical fluctuations.

TRMC methods are based on a fractional step approach, just as DSMC scheme, the difference being in the treatment of the collision step.

We give here a very brief description of TRMC methods. For a more detailed description see, for example, [10–12]. For a review of several techniques for the numerical solution of the Boltzmann equation see, for example, [13].

Consider the space homogeneous Boltzmann equation for the Maxwellian molecules

$$\frac{\partial f}{\partial t} = Q_+(f, f) - \mu f \tag{3}$$

where Q_+ denotes the gain term, and μ is the constant coefficient of the loss term. Formally, the solution of Eq. (3) can be written as

$$f(v, t) = \sum_{k=0}^{\infty} (1 - \tau)\tau^k f_k(v) \tag{4}$$

where $\tau = 1 - \exp(-\mu t)$ denotes the *relaxed time*, while the functions f_k can be computed recursively by the relation

$$f_{k+1} = \frac{1}{k+1} \sum_{h=0}^{k} \frac{1}{\mu} Q_+(f_h, f_{k-h})$$

with $f_0(v) = f(v, 0)$. Note that in this representation, all coefficients in τ are positive and sum to one, and the functions f_k are normalized so that their integrals are equal to the integral of f_0.

It can be proved that, under some quite general assumption, the functions f_k satisfy the property

$$\lim_{k\to\infty} f_k(v) = M(v)$$

where $M(v)$ denotes the Maxwellian with the same moments (density, mean velocity and energy) as f_0. In view of this property, TR schemes are obtained by truncating Wild's sum (4), replacing all high order functions f_k by Maxwellian, and advancing by a finite time step Δt. Such a time relaxed scheme of order m takes the form

$$f^{n+1}(v) = \sum_{k=0}^{m} A_k(\tau) f_k^n(v) + A_{m+1}(\tau) M^n(v) \tag{5}$$

where the coefficients $A_k(\tau)$, $k = 0, \ldots, m+1$, are probabilities (they are non-negative and sum to one). They satisfy the property $A_k(1) = \delta_{k,m+1}$, where δ denotes the Kronecker symbol. This property ensures that as $\mu\Delta t \to \infty$ the distribution function f^{n+1} is projected to a Maxwellian, and the splitting method becomes a kinetic scheme for the Euler equations of gas dynamics.

Time relaxed Monte Carlo methods are obtained by the probabilistic interpretation of Eq. (5). For example, for $m = 2$, a particle sampled from f^{n+1} is obtained as follows:

- with probability A_0 it is sampled from $f_0^n(v) \equiv f^n(v)$, i.e. no collision,
- with probability A_1 it is sampled from f_1^n, i.e. it is obtained as the outcome of a collision with a particle sampled from f_0^n,
- with probability A_2 it is sampled from f_2^n, i.e. it is obtained as the outcome of the collision between a particle sampled from f_0^n and a particle sampled from f_1^n,
- with probability A_3 it is sampled from a Maxwellian.

The scheme can be made conservative by sampling particle pairs rather than individual particles, and by using a suitable conservative sampling from Maxwellians. The scheme can be generalized to hard sphere molecules or to other collisional mechanisms by replacing real collisions by dummy collisions, and using an estimate on the collision frequency, just as in standard DSMC.

Several extensions and generalizations of such basic scheme have been proposed. See, for example, [11] and [12] for recent developments of TRMC schemes.

3.6. Hard sphere molecular dynamics

The Molecular Dynamics method for hard sphere molecules has been described in detail by M.P. Allen and D.J. Tildesley [14]. They also supplied the demonstration computer program (in FORTRAN 77) which, after suitable modifications, was used in the present project.

In the calculations, the medium was modeled as an ensemble of identical hard spheres of finite diameter. Such spherical molecules moved freely in space and collided with each other when they met. At each step of the calculation the collision, nearest in time, was located (i.e. the colliding molecules were selected and the time interval until their collision was found). All particles were then moved forward over that time interval and, finally, the collision itself was calculated. This procedure was repeated as many times as necessary.

To begin calculations, the Maxwellian distribution of molecular velocities was imposed in a standard way [14]. To avoid the unallowed overlaps, the molecules (of finite diameter) were initially distributed in space in some regular fashion and then allowed to move and collide for sufficiently long time to form the desired equilibrium distribution. After that, suitable modification of the velocity distribution was introduced (like e.g. imposing the macroscopic velocity for shock generation) and the actual calculations were started.

To calculate the relaxation process, 64 000 molecules of 0.341 nm diameter (the value for Argon) were placed in a cubic box of 80 nm dimension.

We remark here that, at variance with all the other methods, Molecular Dynamics is not a numerical method for the Boltzmann equation; rather, it is a tool that simulates the behavior of a set of N elastic spheres. It could be used, in principle, to test the validity of the Boltzmann equation itself.

To calculate the shock wave structure, 160 000 molecules of the same diameter were placed in a cuboidal box of dimensions: 800 nm × 40 nm × 40 nm.

3.7. Discrete velocity method

Discrete Velocity (DV) method as well as described below Discrete Velocity Monte Carlo (DVMC) method are based on the discrete velocity approximation of the collision operator

$$Q(f,f)(\mathbf{v}_i) \approx \sum_{\mathbf{v}_j \in \mathbf{v}_i + \Delta v \mathbb{Z}^3} \sum_{(k,l)} \Gamma_{ij}^{kl} (f_k f_l - f_i f_j) \tag{6}$$

on the discrete regular lattice $\Delta v\mathbb{Z}^3$ in the velocity space $\mathbb{R}^3$ with $\mathbf{v}_i \in \Delta v\mathbb{Z}^3$ and Δv denoting the step of the velocity lattice. In (6) the second sum denotes the summation over all k and l such that $\mathbf{v}_k$ and $\mathbf{v}_l$ constitute post-collision velocities for particles with pre-collision velocities $\mathbf{v}_i$ and $\mathbf{v}_j$. The coefficients Γ_{ij}^{kl}, which distinguish both methods, are defined as suitable approximation to the collision kernel (see [15]).

Below we describe briefly a particular method of calculating the discrete velocity approximation (6) used in DV (for a detailed description see [15] and [16]).

First we replace $\Delta v\mathbb{Z}^3$ in (6) by its twice coarser sub-lattice $2\Delta v\mathbb{Z}^3$ and balance the sum by the multiplicative factor 8. Then we perform the summation over a bounded domain V in the lattice $2\Delta v\mathbb{Z}^3$ in a manner similar to the integration in $\mathbb{R}^3$ using the spherical coordinates. If $V(m)$ denotes the set of discrete velocities $\mathbf{v} \in \Delta v\mathbb{Z}^3$ lying on the sphere of radius $\sqrt{m}\,\Delta v$ centered at 0 for $m = 1, 2, \ldots$, we can write

$$\sum_{\mathbf{v}_j \in \mathbf{v}_i + \Delta v\mathbb{Z}^3} \sum_{(k,l)} \ldots \approx 8 \sum_{m=1}^{m_{\max}} \sum_{\mathbf{v}_j \in \mathbf{v}_i + 2V(m)} \sum_{\mathbf{v}_k \in \mathbf{c}_{ij} + V(m)} \ldots \tag{7}$$

where the integer $m_{\max}$ is such that $2\sqrt{m_{\max}}\Delta v$ is the diameter of a finite discrete velocity lattice $\mathbf{I}_N = \{\mathbf{v}_1, \ldots, \mathbf{v}_N\} = V \cap 2\Delta v\mathbb{Z}^3$ used in actual computations and $\mathbf{c}_{ij} = \frac{1}{2}(\mathbf{v}_i + \mathbf{v}_j)$ is the center of the sphere spanned by $\mathbf{v}_i$ and $\mathbf{v}_j$. The above procedure can be accelerated by limiting the number of radii of the spheres $V(m)$ taken in (7) to some m_s such that $1 \leqslant m_s \leqslant m_{\max}$. This acceleration reduces the computational cost of the above numerical method by orders of magnitude without losing much of the accuracy (cf. [16]).

3.8. Discrete velocity Monte Carlo method

In the conservative discrete velocity Monte Carlo method (DVMC) Monte Carlo quadratures are used to compute the collision integral. Below we give a short description of a method described fully in [17].

Let us assume that the velocity space $\mathbb{R}^3$ has been replaced by a bounded domain V with a lattice $\mathcal{V} = V \cap \Delta v\mathbb{Z}^3$. Let $(\mathbf{w}_i, \theta_i, \epsilon_i)$, $i = 1, \ldots, N$, be random points sampled from $\mathcal{V} = [0, R] \times [0, \pi/2] \times [0, 2\pi]$ according to the probability distribution function $\mathcal{P}(\mathbf{w}, \theta, \epsilon)$. Then the Monte Carlo approximation of the collision operator with the collision kernel corresponding to the hard sphere model is given by the following formula

$$Q(f, f)(\mathbf{v}_i) \approx \frac{1}{N} \sum_{j=1}^{N} \frac{1}{\mathcal{P}(\mathbf{w}_j, \theta_j, \epsilon_j)} |\mathbf{v}_i - \mathbf{w}_j| \cos\theta_j \sin\theta_j \big(f(\mathbf{v}_i') f(\mathbf{w}_j') - f(\mathbf{v}_i) f(\mathbf{w}_j) \big)$$

which obviously can be written in a form of the discrete approximation (6) with $\mathbf{v}_i'$, $\mathbf{w}_j'$ being the post-collision velocities.

In general the randomly chosen velocity $\mathbf{w}_j$ and the post-collision velocities $\mathbf{v}_i'$, $\mathbf{w}_j'$ do not belong to the velocity lattice $\mathcal{V}$, and therefore one has to use an interpolation to obtain the values of $f(\mathbf{w}_i)$, $f(\mathbf{v}_k')$ and $f(\mathbf{w}_i')$. The various Monte Carlo formulas for the evaluation of the collision integral are obtained by defining an appropriate probability distribution function $\mathcal{P}$ and by applying special techniques reducing the variance.

In our calculations we assumed the uniform distribution $\mathcal{P}(\mathbf{w}_i, \theta_i, \epsilon_i) = 1/(|V|\pi^2)$ where $|V|$ denotes the volume of the computational velocity domain.

Methods based on Monte Carlo quadratures are not conservative. Thus a correction technique which enforces the conservativeness was introduced (see [17]). The numerical solution f^{**} obtained in the relaxation stage of the n-th time step t_n of the splitting procedure is corrected by adding a term $f^{**} \sum_{i=0}^{4} \alpha_i \psi_i$, where $\psi_0(\mathbf{v}) = 1$, $\psi_i(\mathbf{v}) = v_i$ for $i = 1, 2, 3$, and $\psi_4(\mathbf{v}) = |\mathbf{v}|^2$. The numbers α_i are determined by requiring that the (discretized) conservation laws

$$\sum_{k \in \mathbf{I}} \psi_j(\mathbf{v}_k) f_k^{**}(t_{n+1}) \left(1 + \sum_{i=0}^{4} \alpha_i \psi_i(\mathbf{v}_k) \right) = \sum_{k \in \mathbf{I}} \psi_j(\mathbf{v}_k) f_k^{*}(t_{n+1})$$

are satisfied for $j = 0, \ldots, 4$.

3.9. FFT method

The FFT method is a spectral scheme. A spectrally accurate scheme on uniform grid in velocity has been presented in [18] for the space homogeneous Boltzmann equation, and applied to the space non-homogeneous problems in [19]. Such method has the advantage of being very accurate and rather efficient compared to other deterministic schemes. However, the scheme on a uniform grid has difficulty in performing the computation of a shock with large Mach number. The main reason is that the temperature and mean velocity on both sides of the shock are very different and a single grid is not sufficient for an adequate treatment of the problem. For this reason, and in order to be able to treat problems which admit discontinuous distribution functions, a new FFT method has been derived. It uses a version of the standard Fast Fourier Transform to approximate the collision integral on non-uniform adaptive grids in the velocity space. The method is especially useful in effective approximation of discontinuous solutions. Below we briefly describe the method (for a detailed description see [20].

The computation of the gain term $Q^+(f,f)$ and the collision frequency $q^-(f)$ is based on a pseudodifferential representations of these operators using Fourier transform $F(f)=\hat{f}_m$ of the distribution function f:

$$\begin{aligned} Q^+(f,f)(\mathbf{v}) &= F_l^{-1}(\mathbf{v})F_m^{-1}(\mathbf{v})\big[\hat{f}_l\hat{f}_m\hat{B}(\mathbf{l},\mathbf{m})\big],\\ q^-(f)(\mathbf{v}) &= F_m^{-1}(\mathbf{v})\big[\hat{f}_m\hat{B}(\mathbf{m},\mathbf{m})\big] \end{aligned} \tag{8}$$

where

$$\hat{B}(\mathbf{l},\mathbf{m}) = \int\limits_{\mathbb{R}^3}\int\limits_{S^2} B(|\mathbf{u}|,\theta)\exp\left(2\pi\imath\left(\frac{\mathbf{l}+\mathbf{m}}{2},\mathbf{u}\right)\right)\exp\left(2\pi\imath|\mathbf{u}|\left(\frac{\mathbf{m}-\mathbf{l}}{2},\omega\right)\right)\mathrm{d}\omega\,\mathrm{d}\mathbf{u}.$$

An effective approximate version of the fast Fourier transform (see [21]) is used on the non-uniform grid for the distribution function f. It makes the algorithm robust. The amount of computations is of order $N^3\log(N)+N_p$. Here N is the number of Fourier modes along one coordinate direction used for the approximation of the smooth functions $Q^+(f,f)$ and $q^-(f)$. N_p is the number of points in the non-uniform grid where f is defined.

To efficiently evaluate the gain part (8) we use the fact that in our case $\hat{B}$ depends only on $|\mathbf{l}+\mathbf{m}|$ and $|\mathbf{l}-\mathbf{m}|$. Hence defining $T(|\mathbf{p}|,|\mathbf{q}|) := \hat{B}(\mathbf{l},\mathbf{m})$ with $\mathbf{p}=\mathbf{l}+\mathbf{m}$ and $\mathbf{q}=\mathbf{l}-\mathbf{m}$ we get the following approximation

$$Q^+(f,f)(\mathbf{v}) \approx \sum_{\mathbf{p}} F(\mathbf{p})\,\mathrm{e}^{-2\pi\imath(\mathbf{p},\mathbf{v})}$$

where $F(\mathbf{p})=\sum_{\mathbf{q}}\hat{f}_{\frac{p+q}{2}}\hat{f}_{\frac{p-q}{2}}T(|\mathbf{p}|,|\mathbf{q}|)$.

The FFT scheme, which is a spectral method to some extend, conserves only mass – momentum and energy are not conserved. The correction technique enforcing the conservation property used here is analogous to the one in DVMC method.

4. Numerical tests

4.1. Relaxation process

In this subsection we give the results of an example of the relaxation problem calculated using six numerical methods (DSMC, DV, DVMC, TRMC2, FFT, MD).

We study the relaxation of the second moment of solution of the homogeneous Boltzmann equation. As initial data we take the sum of two Maxwellians shifted in the xz-direction.

The time step used in numerical tests was $\Delta t = 0.01$ for TRMC2 and FFT and $\Delta t = 0.02$ for other methods and the computations were performed up to time $T=4$. For the DSMC and TRMC2 calculations, 50 000 particles were taken with averaging the results over 50 runs. The number of velocities was 16 for the DV and 15 for the DVMC in each direction and the velocity grid step $\Delta v = 1.0$. The Monte Carlo quadrature with 200 points was used in the DVMC.

In Fig. 3 we present the graph of the xz-moment vs. time. All the curves are very similar and differences are negligible. The relative error measured by the L^1 distance between the lowest and the highest relaxation rate is approx. 2.5%.

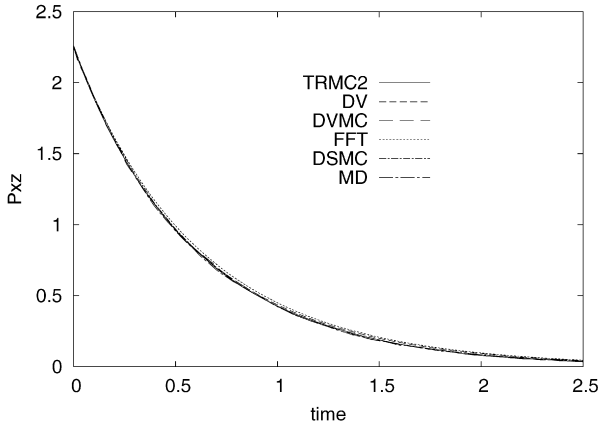

Fig. 3. Relaxation problem: xz-moment.

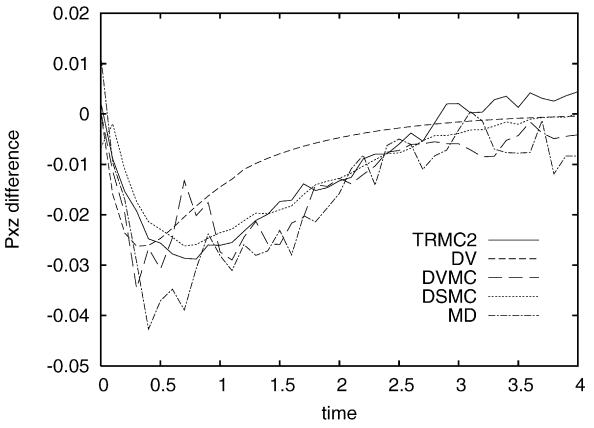

Fig. 4. Absolute error for relaxation problem.

To make the comparison more transparent we show in Fig. 4 the differences between FFT curve taken as a reference value and all other curves. This can be seen as a measure of an absolute error. Several remarks are appropriate at this point. First, the time interval is larger than in Fig. 3 to show how the error behaves when the xz-moment approaches equilibrium. Second, the inspection of the data shows that the MD method gives slightly higher relaxation rate compared to the other methods, particularly when the system is far from equilibrium. But even for this largest deviation the relative error is below 2.5%.

Finally, we should observe the smooth curve corresponding to DV calculations contrary to all other curves. This is related to the nature of the numerical methods we have used. The FFT and DV methods are fully deterministic algorithms for the Boltzmann equation. As such they produce smooth results. The other methods use randomness at certain level (MD method is in fact not random but averaging over large number of individual trajectories, which gives similar result). The jumps we observe in Fig. 4 are the traces of white noise which is immanent to random methods. Let us observe however, that the DSMC and TRMC2 methods produce much smoother curves than the MD and DVMC methods. This can suggest that the number of samples used for averaging in the latter methods was to small.

4.2. Shock wave structure

As a test for the methods in the non-homogeneous case we consider 1D shock wave propagation problem. The calculations have been performed for DSMC, DV, DVMC, TRMC2 and MD methods.

The numerical calculations were obtained with the physical space step $\Delta x = 0.25$. The calculations for DV and DVMC were performed with the velocity grid step $\Delta v = 1.0$ with 15 velocities in each direction and the time step $\Delta t = 1/30$. (All values in the dimensionless units introduced in Section 3.1.)

To compare results we calculated normalized density and temperature:

$$n = \frac{\rho - \rho_1}{\rho_2 - \rho_1}, \qquad \theta = \frac{T - T_1}{T_2 - T_1}.$$

In Figs. 5 and 6 we show the normalized density and temperature profiles, respectively, for the numerical methods and for the experimental data (only the density profile for experimental data). One can see a good agreement between all shock profiles. The density level behind the shock, as obtained from Molecular Dynamics simulation, is remarkably below 1 (contrary to the normalization). This is due to the finite volume of the molecules: theoretical density ratio across the shock, used here, has been calculated for the ideal case of point mass (zero volume) molecules.

To make the visual comparison more transparent we have chosen the most distant calculations (DV and TRMC2) and compared them with the experimental profile for density. It is still visible that the agreement is quite reasonable (Fig. 7).

To compare the numerical methods with the experiment we use parameters introduced in Section 1. Since only the density profile is available for the experiment, we compared the shift between the temperature and density profiles for the numerical results only.

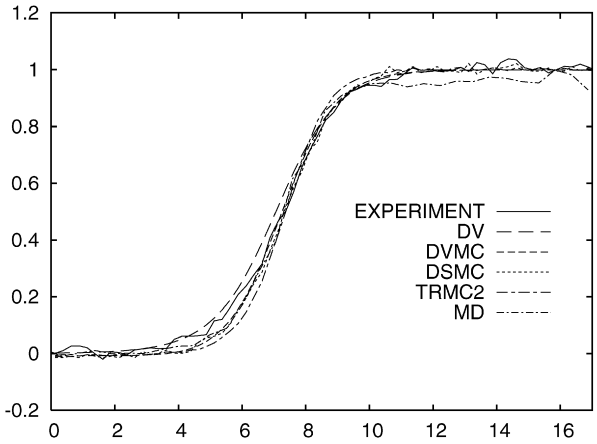

Fig. 5. The density profiles of the shock wave.

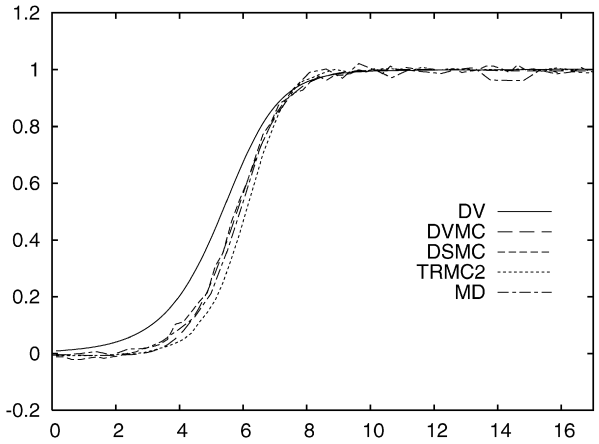

Fig. 6. The temperature profiles of the shock wave.

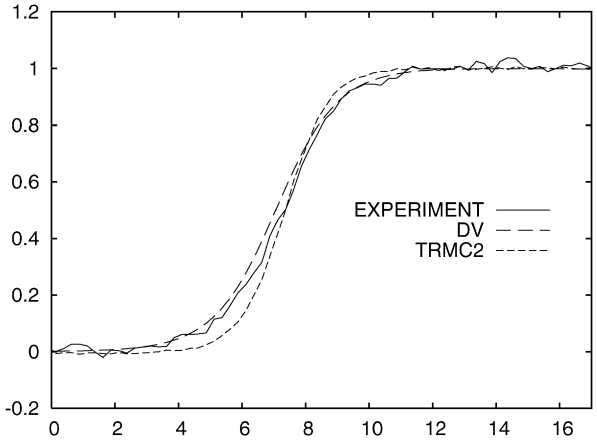

Fig. 7. The density profiles for experimental, DV and TRMC2 data.

Table 1
Shock wave width and shift

	Density	Temperature	Shift
DSMC	3.462	2.974	1.583
DV	3.943	3.734	1.714
DVMC	3.428	3.020	1.447
TRMC2	2.782	2.620	1.280
MD	3.335	2.752	1.451
Experiment	3.840	–	–

In Tables 1 and 2 we present the quantitative results of comparison for the numerical methods and the experiment. In Table 1 we give the width of the shock (the maximum-slope shock thickness) for density and temperature profiles and the shift between them.

To calculate the shock thickness we have taken intervals containing 60% of the shock jump considered, i.e. j_1 is the largest index for which $n_j < 0.2$ and j_2 is the smallest index for which $n_j > 0.8$. The normalized density is then fitted by a cubic polynomial in this interval. The maximum slope is then determined from this polynomial. The inverse of the maximum slope is the thickness of the shock density profile. The same procedure has been used for the temperature profile.

Table 2
Geometric shape factors

	A_1	A_2	Q
DSMC	0.5172	0.6443	0.8028
DV	0.6947	0.7350	0.9451
DVMC	0.5160	0.6008	0.8588
TRMC2	0.4689	0.5811	0.8070
MD	0.5201	0.7201	0.7222
Experiment	0.7316	0.6667	1.0970

There is a good agreement in the shock density width between the DSMC and DVMC methods, while TRMC2 gives higher slope and DV the smallest. The temperature profiles behave very similarly to the density profiles: still TRMC2 has the highest slope and DV the smallest, and there is a large similarity between DSMC and DVMC profiles. DSMC and DVMC give a similar shift between the density and temperature profiles, while TRMC2 gives the smallest shift and DV the largest.

To calculate the geometric factor we have to find exact position at which $n = 0.5$. This has been done by fitting the profile in the interval $0.4 < n < 0.6$ by a cubic polynomial $x = q_3(n)$ and setting $x_M = q_3(0.5)$. The two areas have been obtained by summation from the discrete density profile with a second order correction for the contribution of the cell containing x_M. The geometric shape factors values are given in Table 2.

5. Conclusions

Qualitative agreement between the results obtained by different calculation methods seems to be quite satisfactory. Also the differences from experimental data are not very substantial. On the other hand, careful analysis of observed differences cannot be neglected. First, we observe that DV method gives more diffuse results. This is particularly well visible on the temperature profile of the shock wave but can be also observed on the density profile and for the relaxation calculations. This diffusivity can be attributed to the low resolution of applied grid, i.e. decreasing the time step and increasing the number of grid points in velocity space can eliminate this problem. The numerical complexity of DV method shows however that applying this method with a fine grid is too expensive for practical calculations. On the other hand DV calculations are in best agreement with the experimental data for the density profile (compare the shock wave thickness and the geometric shape factors).

Methods using Monte Carlo algorithms seem to be in better agreement with each other. We remark here that the computations have been obtained by different research groups, using different implementations, and it is likely that some of the differences can be attributed to minor implementation details (e.g. setting of the initial and boundary conditions), which can have a small influence on the final outcome. We tried to minimize such effects by exchange visits among the researchers of the various groups.

Still the differences between any of these methods and experiment is of order 20–25% (shock wave thickness and geometric shape factors). Certainly, these disagreements can be attributed to the model of particle interactions. In all calculations we have used the hard sphere model which is quite distant from real interactions (Lennard–Jones potential). But comparing only the results of different calculations (with DV method excluded) we observe differences of 5% for geometric shape factors and up to 20% for the shock thickness and the profile shift. Very remarkable is also the behavior of the shape factor Q. In all calculations we obtained $Q < 1$ but the experiment gives $Q > 1$.

Very accurate solutions of the Boltzmann equation are obtained by the use of spectral methods. The method used by Filbet and Russo [19] gives spectral accuracy in velocity, second order in time and third order in space. The evaluation of the collision term by spectral methods can be performed by fast algorithms [22], which makes such methods even more competitive. However, for large Mach number, the method is expensive if the same grid in velocity space is used in the whole computational domain. For this reason we did not include the method in the comparison, and we used the FFT method – a spectral method which uses an adaptive grid in velocity [20] – which is more effective for high Mach number, even if it is not spectrally accurate.

One of the important question which arises when we compare different numerical methods is the computational efficiency. The results we presented in the paper were obtained by the different research groups. Hence we could not take the exact computer time as a measure of computational efficiency. Instead we decided to compare the relative

order of computational time for the more expensive 1D case (see Section 4.2): we estimated the time the calculation of each method would take on a reference PC computer with Pentium 4 3.06 GHz processor. The most time consuming was MD method (56 hours) and DV method was roughly 10 times quicker (6 hours). The Monte Carlo simulation methods (TRMC2 and DSMC) computational time was nearly the same (1 hour), while the quickest method was DVMC (10 minutes).

In conclusion we can say that the different calculation methods using kinetic approach for rarefied gasdynamic problems give results which can differ up to 20–25%. This is not only in the case of a different mathematical formulation of the problem, but also when the same mathematical problem is solved by different algorithms (compare differences between DSMC and TRMC2 calculations). These calculations show that there is no clear superior method. Different methods seem to catch different features of the rarefied flow described by the Boltzmann equation. Hence kinetic algorithms for rarefied gas dynamic problems, although well advanced, still require further careful development and analysis.

Acknowledgements

This work was partially supported by EU in the frame of FP5 network HYKE (contract no. HPRN-CT-2002-00282).

References

[1] J.M. Reese, Burnett predictions of hypersonic rarefied gas shockstructure: comparison of theory with experiment, in: Proc. 21st ISSW, Australia, 1997.
[2] I.A. Graur, T.G. Elizarova, J.C. Lengrand, Calculation of shock structure based on QGD model with multiple translational temperatures, in: Proc. 21st ISSW, Australia, 1997.
[3] E.P. Muntz, D.A. Erwin, G.C. Pham-Van-Diep, A review of the kinetic detail required for accurate predictions of normal shock waves, in: A.E. Beylich (Ed.), Proc. XVII RGD Symp., VCH, 1991, pp. 198–206.
[4] Shock tube of the IFTR, Prace IPPT 47/1976, 1976 (in Polish).
[5] H.S. Ballard, D. Venable, Shock front thickness measurements by an electron beam technique, Phys. Fluids 1 (3) (1958) 225–229.
[6] W. Fiszdon, R. Herczynski, Z. Walenta, The structure of a plane shock wave of a monoatomic gas. Theory and experiment, in: Proc. IX RGD Symp., Goettingen, 1974.
[7] G.B. Whitham, Linear and Nonlinear Waves, J. Wiley, New York, 1974.
[8] G.A. Bird, Molecular Gas Dynamics, Clarendon Press, Oxford, 1976.
[9] V.E. Yanitskiy, O.M. Belotserkovskiy, The statistical method of particles in cells for the solution of problems of the dynamics of a rarefied gas, Part I, Zh. Vychisl. Mat. Mat. Fiz. 15 (1975) 1195–1208.
[10] L. Pareschi, G. Russo, Time relaxed Monte Carlo methods for the Boltzmann equation, SIAM J. Sci. Comput. 23 (2001) 1252–1272.
[11] L. Pareschi, S. Trazzi, Numerical solution of the Boltzmann equation by Time Relaxed Monte Carlo (TRMC) methods, Int. J. Numer. Methods Fluids 48 (2005) 947–983.
[12] L. Pareschi, B. Wennberg, A recursive Monte Carlo method for the Boltzmann equation in the Maxwellian case, Monte Carlo Methods Appl. 7 (2001) 349–358.
[13] L. Pareschi, G. Russo, An introduction to the numerical analysis of the Boltzmann equation, Rov. Mat. Univ. Parma 7 (4) (2005) 145–250.
[14] M.P. Allen, D.J. Tildesley, Computer Simulation of Liquids, Clarendon Press, Oxford, 1987.
[15] A. Palczewski, J. Schneider, A.V. Bobylev, A consistency result for discrete velocity model of the Boltzmann equation, SIAM J. Numer. Anal. 34 (1997) 1865–1883.
[16] T. Płatkowski, W. Waluś, An acceleration procedure for discrete velocity approximation of the Boltzmann collision operator, Comp. Math. Appl. 39 (2000) 151–163.
[17] V.V. Aristov, F.G. Tcheremissine, Direct numerical solutions of the kinetic Boltzmann equation, Comp. Center of Russ. Acad. of Sci., Moscow, 1992.
[18] L. Pareschi, G. Russo, Numerical solution of the Boltzmann equation I: spectrally accurate approximation of the collisional operator, SIAM J. Numer. Anal. 37 (2000) 1217–1245.
[19] F. Filbet, G. Russo, High order numerical methods for the space non-homogeneous Boltzmann equation, J. Comput. Phys. 186 (2003) 457–480.
[20] A. Heintz, P. Kowalczyk, R. Grzibovskis, Fast numerical method for the Boltzmann equation on non-uniform grids, Preprint 2004:22, Chalmers University of Technology and Göteborg University, Göteborg, 2004.
[21] G. Beylkin, On the fast Fourier transform of functions with singularities, Appl. Comput. Harmon. Anal. 2 (1995) 363–381.
[22] C. Mouhot, L. Pareschi, Fast algorithms for computing the Boltzmann collision operator, Math. Comp. 75 (2006) 1833–1852.
[23] V.E. Yanitskiy, O.M. Belotserkovskiy, The statistical method of particles in cells for the solution of problems of the dynamics of a rarefied gas, Part II, Zh. Vychisl. Mat. Mat. Fiz. 15 (1975) 1553–1567.